Wannier basis method for the Kolmogorov-Arnold-Moser effect in quantum mechanics

Chao Yin (尹超) ⓘ,[1] Yu Chen (陈宇),[2] and Biao Wu (吴飙) ⓘ[1,3,4]

[1]*International Center for Quantum Materials, School of Physics, Peking University, Beijing 100871, China*
[2]*Center for Theoretical Physics, Department of Physics, Capital Normal University, Beijing 100048, China*
[3]*Collaborative Innovation Center of Quantum Matter, Beijing 100871, China*
[4]*Wilczek Quantum Center, School of Physics and Astronomy, Shanghai Jiao Tong University, Shanghai 200240, China*

The effect of the Kolmogorov-Arnold-Moser (KAM) theorem in quantum systems is manifested in dividing eigenstates into regular and irregular states. We propose an effective method based on the Wannier basis in phase space to illustrate this division of eigenstates. The quantum kicked-rotor model is used to illustrate this method, which allows us to define the area and effective dimension of each eigenstate to distinguish quantitatively regular and irregular eigenstates. This Wannier basis method also allows us to define the length of a Planck cell in the spectrum that measures how many Planck cells the system will traverse if it starts at the given Planck cell. Moreover, with this Wannier approach, we are able to clarify the distinction between the KAM effect and Anderson localization.

I. INTRODUCTION

There are two contrasting types of motion in classical dynamics. The first type is regular orbits in integrable systems, where there exist N independent conserved quantities (N is the degree of freedom) that restrict motion to an N-dimensional torus in phase space [1]. The second type is irregular motion in chaotic systems, where most orbits explore almost all points in a $(2N - 1)$-dimensional energy surface in the sense of ergodicity and mixing [2]. According to the well-known Kolmogorov-Arnold-Moser (KAM) theorem [3–5], there is a smooth crossover from an integrable system to a chaotic system. Specifically, Kolmogorov, Arnold, and Moser considered a Hamiltonian of the form $H = H_0 + \epsilon H'$, where H_0 is integrable. They found that a subset of the torus solutions under H_0 is deformed and survives under a sufficiently small perturbation $\epsilon H'$, while motion near the unstable tori is chaotic and fills regions with dimensionality $2N - 1$. As a result, the phase space is divided into integrable and chaotic regions, with the measure of the latter growing with ϵ.

As classical dynamics is the semiclassical limit ($\hbar \to 0$) of quantum dynamics, one expects similar KAM effects in quantum mechanics. There has been a great deal of work extending KAM effects to quantum systems [6–14]; in particular, KAM effects in quantum many-body systems have recently become of interest [13,14]. In this paper we focus on cases that have classical limits. In these systems, previous studies have shown that quantum KAM effects are manifested in eigenenergies and eigenfunctions. The eigenenergies and eigenfunctions of KAM-type systems have two parts: a regular part and an irregular part [15–19]. In particular, to quantitatively understand regular and irregular eigenfunctions, there have been serious efforts to compare quantum eigenfunctions to classical orbits in phase space using either the Wigner distribution [17,18] or Husimi distribution [20–22].

In this work we propose a different method to capture the quantum KAM effect, i.e., the division of regular and irregular eigenstates. In our approach, we divide the phase space into Planck cells and assign a Wannier function to each Planck cell [23–25]. These Wannier functions form an orthonormal and complete basis and allow us to project a wave function unitarily to phase space. With this unitary projection, we are able to define for every eigenfunction an area which measures how much phase space the eigenfunction occupies in the phase space. We are also able to define an effective dimension for every eigenfunction. Our numerical results show that the effective dimension of an irregular eigenfunction is the same as the phase space, while a regular eigenfunction has a lower dimension. We are also able to define a length for each Planck cell by projecting the Wannier basis back to the eigenstates. Using numerical evidence, we argue that this length measures how much phase space the long-time quantum trajectory will traverse when starting from the given Planck cell.

We illustrate our method using the quantum kicked rotor (QKR) model, whose classical counterpart, the classical kicked rotor (CKR) [26], is one of the simplest models governed by the KAM theorem. We first consider the case of $\hbar_e/2\pi$ being a rational number, where $\hbar_e$ is the effective Planck constant. Then we extend our discussion to generic $\hbar_e$ and show the distinction between KAM effects and Anderson localization.

II. THE QKR MODEL AND WANNIER BASIS APPROACH

A. The QKR model

The dimensionless Hamiltonian of the QKR can be written as [25]

$$\hat{H} = \frac{\hat{p}^2}{2} + K \cos \hat{x} \sum_{j=-\infty}^{+\infty} \delta(t - j), \qquad (1)$$

where $\hat{p}$ is the dimensionless angular momentum operator, $\hat{x}$ is the angular coordinate operator, t is dimensionless time, and K is the kicking strength. In the coordinate representation, $\hat{p} = -i\hbar_e(\partial/\partial x)$, where $\hbar_e$ is the dimensionless effective Planck constant. The dimensionless Schrödinger equation is $i\hbar_e(\partial/\partial t)|\Psi\rangle = \hat{H}|\Psi\rangle$. Note that for a real rotor with a moment of inertia I and driving period T, the effective Planck constant is given by $\hbar_e = \hbar T/I$.

The evolution operator over one period is

$$\hat{U} = \exp\left(-\frac{i}{2}\frac{\hat{p}^2}{\hbar_e}\right)\exp\left(-\frac{i}{\hbar_e}K\cos\hat{x}\right). \quad (2)$$

For this system, the momentum basis $\langle x|n\rangle = e^{inx}$ (n is an integer) is the most convenient. The matrix elements of $\hat{U}$ are given by

$$U_{n'n} \equiv \langle n'|\hat{U}|n\rangle = (-i)^{n-n'}J_{n-n'}\left(\frac{K}{\hbar_e}\right)\exp\left(-\frac{in'^2\hbar_e}{2}\right), \quad (3)$$

where $J_{n-n'}(K/\hbar_e)$ is a Bessel function of the first kind. The eigenstates of the Floquet operator $\hat{U}$ in this periodically driven system play the same role as energy eigenstates in a time-independent system.

In the following discussion, unless specified otherwise, we focus on the case that $\hbar_e/2\pi$ is rational, that is, $\hbar_e = 2\pi M/N$, where M and N are coprime positive integers [27]. This is called quantum resonance [28]. In this work, for simplicity, we assume that N is even. For even N, we find that $U_{n+N\ell,n'+N\ell} = U_{nn'}$ ($l = 0, \pm 1, \ldots$), which reflects a translational symmetry in p space (see Appendix A for details). This means that an eigenstate $|\phi\rangle$ of the unitary operator $\hat{U}$ must be of the form of Bloch states

$$\phi(s + N\ell) \equiv \langle s + Nl|\phi\rangle = e^{-il\theta}\phi_\theta(s), \quad 0 \leqslant \theta < 2\pi, \quad (4)$$

where $s = 1, \ldots, N$; $l = 0, \pm 1, \ldots$; and θ is a Bloch wave vector along p. This shows that all eigenstates are extended in p space, and thus have an infinite expectation value of kinetic energy. Moreover, $\phi_\theta(s)$ is the eigenstate of an $N \times N$ matrix V_θ,

$$\sum_{s'=1}^{N} V_\theta(s,s')\phi_\theta(s') = e^{-i\omega_\phi}\phi_\theta(s), \quad (5)$$

where ω_ϕ is the quasienergy of $|\phi\rangle$ and

$$V_\theta(s,s') \equiv \sum_{\ell'=-\infty}^{+\infty} U_{s,s'+N\ell'}e^{-i\ell'\theta}. \quad (6)$$

This suggests that the Hilbert space can be reduced naturally to finite dimensions without truncation, which is one of the benefits of the resonance condition. Our results have little dependence on the Bloch wave vector θ, which is also shown in [27]. Therefore, we will always choose $\theta = 0$ and denote V_θ simply by V and ϕ_θ by ϕ. The second benefit with the resonance condition is that the quantum phase space is naturally constructed, while there is some insignificant ambiguity when $\hbar_e$ is generic, which we will see in the next section.

B. Construction of quantum phase space

In order to compare the quantum dynamics with its classical counterpart, we construct a quantum phase space. This is accomplished by dividing the classical phase space into Planck cells and assigning a Wannier function to each Planck cell [23–25]. These Wannier functions are localized in their corresponding Planck cells and form a complete basis for the Hilbert space. In this work, we follow the method in Ref. [25]. Suppose $N = N_x N_p$, where N_x and N_p are integers. The Wannier function is constructed as

$$|\mathcal{X}, \mathcal{P}\rangle = \frac{1}{\sqrt{N_x}}\sum_{n=1}^{N_x}\exp\left(-i\frac{2\pi\mathcal{X}n}{N_x}\right)|n + \mathcal{P}N_x\rangle, \quad (7)$$

where $\mathcal{X} = 0, 1, \ldots, N_x - 1$ and $\mathcal{P} = 0, 1, \ldots, N_p - 1$. It is straightforward to show that the new basis is orthonormal and complete. From Eq. (7) it is clear that $|\mathcal{X}, \mathcal{P}\rangle$ is localized in p space. Moreover, it is also localized in x space because its x representation is given by

$$\langle x|\mathcal{X}, \mathcal{P}\rangle = \frac{1}{\sqrt{2\pi N_x}}\frac{\sin(N_x x/2)}{\sin\left(\frac{x}{2} - \pi\frac{\mathcal{X}}{N_x}\right)}$$
$$\times \exp\left[\frac{i}{2}(2\mathcal{P}N_x - N_x + 1)x - i\pi\frac{\mathcal{X}}{N_x}\right], \quad (8)$$

whose norm is plotted in [25].

Thus, any quantum state $|\psi\rangle$ has a phase-space representation $|\psi\rangle = \sum|\mathcal{X}, \mathcal{P}\rangle\langle\mathcal{X}, \mathcal{P}|\psi\rangle$ and $P_{\mathcal{X},\mathcal{P}} = |\langle\mathcal{X}, \mathcal{P}|\psi\rangle|^2$ is the probability for $|\psi\rangle$ to be in Planck cell $(\mathcal{X}, \mathcal{P})$. We emphasize that this basis can be constructed as long as one has the classical action-angle pairs (p, x), where x has a periodic boundary condition. If the natural coordinate of the classical system is not the angle variable, one can also numerically obtain an orthonormal and complete basis of Wannier functions efficiently [24].

If we push the limit $N_x, N_p \to \infty$ keeping M constant, we get an unlimited resolution in the phase space $\hbar_e \to 0$; it can be proved that the quantum dynamics will be reduced to the standard map for the CKR [25], that is, $\langle\mathcal{X}, \mathcal{P}|\hat{V}|\mathcal{X}_0, \mathcal{P}_0\rangle$ will vanish unless

$$\bar{\mathcal{P}} = \bar{\mathcal{P}}_0 + \frac{K}{2\pi M}\sin(2\pi\bar{\mathcal{X}}_0), \quad (9)$$

$$\bar{\mathcal{X}} = \bar{\mathcal{X}}_0 + M\bar{\mathcal{P}}, \quad (10)$$

where $\bar{\mathcal{X}} = \mathcal{X}/N_x \in [0, 1]$ and $\bar{\mathcal{P}} = \mathcal{P}/N_p \in [0, 1]$. Taking $\bar{\mathcal{P}}' = M\bar{\mathcal{P}}$, one can see that the map for the pair $(\bar{\mathcal{P}}', \bar{\mathcal{X}})$ is exactly the standard map in the CKR. The effect of M is to divide the phase space $(0 < \bar{\mathcal{X}} < 1, 0 < \bar{\mathcal{P}} < 1)$ into M phase spaces of the standard map along the $\bar{\mathcal{P}}$ direction. Each of the M phase spaces will be referred to as a sub-phase-space in this paper.

C. Area and effective dimension of eigenstates

In the CKR model, the Hamiltonian is nonintegrable as long as K is nonzero, but even in the region $1 < K < 5$, there is still a finite portion of quasiperiodic trajectories surviving under the strong kicking strength. Under these K, the classical phase space is divided clearly into two kinds of regions: some small integrable islands and a large chaotic sea [29].

If an initial state lies in the chaotic region, it will explore almost everywhere in the chaotic sea during its long-time dynamics. On the contrary, if an initial state lies on one integrable island, it will remain on one trajectory which forms a one-dimensional line inside the integrable island. Thus we can tell whether a trajectory is integrable or chaotic by its area in the phase space. In practice, we divide the phase space into $N_c \times N_c$ cells and define the coarse-grained area of a trajectory by the number of cells passed through by the trajectory. Then the area of a chaotic trajectory will be proportional to N_c^2, while that of an integrable trajectory will be proportional to N_c, which gives a rigorous division in the limit $N_c \to \infty$.

As the quantum phase space is naturally coarse grained by Planck cells, we can define the area of an eigenstate, which serves as a criterion to distinguish integrable and chaotic eigenstates. We define the area $\mathcal{A}$ of a given state $|\psi\rangle$ as

$$\mathcal{A}(|\psi\rangle) = \left(\sum_{\mathcal{X}, \mathcal{P}} |\langle \mathcal{X}, \mathcal{P} | \psi \rangle|^4 \right)^{-1}. \quad (11)$$

It is clear that each Wannier basis has area $\mathcal{A}(|\mathcal{X}, \mathcal{P}\rangle) = 1$; if $|\psi\rangle$ is equally distributed in N_ψ Planck cells while it has no overlap with other cells, its $\mathcal{A}$ will be equal to N_ψ. Thus, this definition can reflect the extent of expansion of the state in the quantum phase space. Note that this quantity is called the inverse participation ratio, defined in a slightly different context [30–34].

We expect, in the semiclassical limit $N_x, N_p \to \infty$ with N_x/N_p constant, $\mathcal{A} \propto N = N_x N_p$ for chaotic eigenstates and $\mathcal{A} \propto \sqrt{N}$ for integrable ones. Since $\hbar_e \propto 1/N$, we define the effective dimension of each eigenstate ϕ,

$$D_{\text{eff}}(\phi) = -2 \lim_{\hbar_e \to 0} \frac{\ln \mathcal{A}(\phi)}{\ln \hbar_e}, \quad (12)$$

which will be close to 1 for integrable eigenstates and 2 for chaotic ones. We note that although $\mathcal{A}$ is dependent on the construction details of phase space, D_{eff} is universal. Instead of looking at the Husimi distribution of each eigenstate to determine which type that state belongs to, we can make the discrimination directly from the value of its area or effective dimension by means of the Wannier phase space, which enables us to make the classification of all eigenstates, just as in classical mechanics, where a single Poincaré section can depict the behavior of all orbits.

In the definition of D_{eff}, one needs to relate eigenstates at different $\hbar_e$. This is not straightforward, as the number of all eigenstates varies with $\hbar_e$. To relate eigenstates, we sort all eigenstates by their area and get the index $\ell_{\mathcal{A}(\phi)} \in \{1, \ldots, N\}$ for each ϕ. Then we label each ϕ by its normalized position $\ell_\phi \equiv \ell_{\mathcal{A}(\phi)}/N \in [0, 1]$. Finally, two states at different $\hbar_e$ are regarded as the same eigenstate if they have the same ℓ_ϕ.

III. MANIFESTATION OF THE KAM EFFECT IN THE QKR

A. Quantum resonance: $\hbar_e = 2\pi/N_x^2$

In this section, we present our main results using the Wannier basis to investigate the classification of eigenstates in the system. We first consider the simplest case $\hbar_e = 2\pi/N_x^2$.
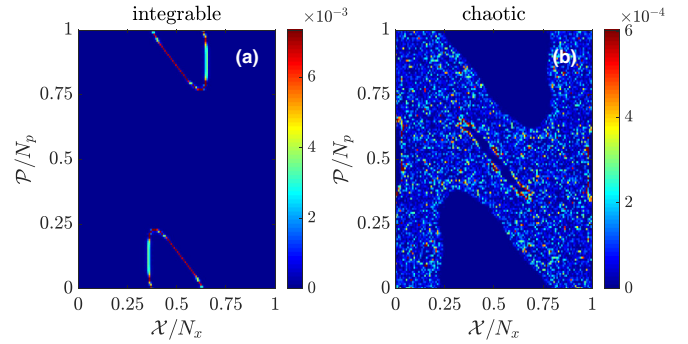

FIG. 1. Phase-space representation of (a) an integrable eigenstate and (b) a chaotic eigenstate at $K = 2$ and $N_x = N_p = 128$. The value of each cell is $|\langle \mathcal{X}, \mathcal{P} | \phi \rangle|^2$, where $|\phi\rangle$ is the eigenstate.

As expected, there are two types of eigenstates, and two examples are shown in Fig. 1.

We calculate the area $\mathcal{A}$ for each eigenstate, and there is a sharp step when $\mathcal{A}$ is plotted as a function of the eigenstate index ℓ_ϕ [see Fig. 2(a)]. The step gets sharper when N_x is increased or, equivalently, when $\hbar_e$ is decreased. This sharp step defines a critical value ℓ_ϕ^c. One can roughly say that the eigenstates with $\ell_\phi < \ell_\phi^c$ are integrable and those with $\ell_\phi > \ell_\phi^c$ are chaotic. Moreover, one expects that the area at $\ell_\phi < \ell_\phi^c$ is $\mathcal{A}(\phi)/N \propto 1/N_x$ [see Fig. 2(b)], while $\mathcal{A}(\phi)/N$ tends to a constant at $\ell_\phi > \ell_\phi^c$.

The effective dimension D_{eff} is also calculated and is plotted in Fig. 2(d). As expected, $D_{\text{eff}} = 1$ for eigenstates below ℓ_ϕ^c and $D_{\text{eff}} = 2$ for eigenstates above ℓ_ϕ^c. However, near ℓ_ϕ^c, D_{eff} deviates from both 1 and 2, which may indicate the existence of hierarchial states, described in Ref. [22]. These states correspond to classical orbits which are trapped in the vicinity of the hierarchy of integrable islands for a long
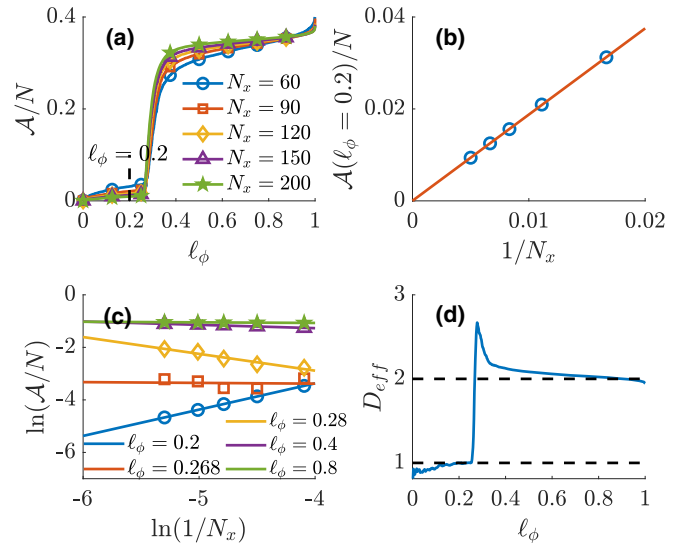

FIG. 2. (a) Plot of $\mathcal{A}(\phi)$ of all eigenstates at different N_x. (b) Plot of $\mathcal{A}(\phi)$ at $\ell_\phi = 0.2$ for different N_x. (c) Logarithmic fitting for five typical ℓ_ϕ. (d) Effective dimension D_{eff} of all eigenstates ℓ_ϕ, where D_{eff} is calculated from the slope of the logarithmic fitting. The parameters are $\hbar_e = \frac{2\pi}{N_x^2}$ and $K = 2$.
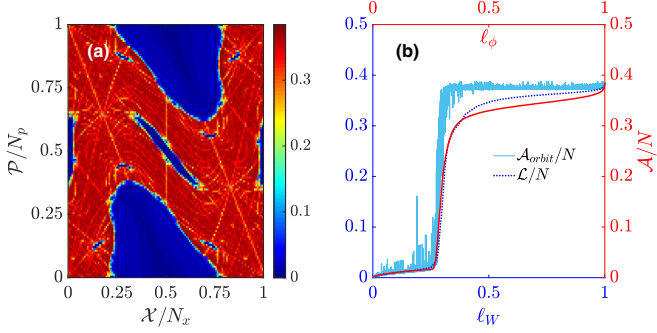
FIG. 3. (a) Length $\mathcal{L}/N$ of each Wannier basis. (b) Sorted area $\mathcal{A}/N$ of each eigenstate (red solid line), sorted $\mathcal{L}/N$ of each Wannier basis (dark blue dotted line), and long-time area $\mathcal{A}_{\text{orbit}}/N$ of them (light blue solid line). Similar to how eigenstates are sorted and labeled by ℓ_ϕ, each Wannier basis is sorted by its length $\mathcal{L}$ and is then labeled by $\ell_W \in [0, 1]$. The parameters for both figures are $K = 2$ and $N_x = N_p = 128$.

time but will finally leak into the chaotic sea. These states will disappear when $\hbar_e \to 0$ [22].

We have projected unitarily one set of basis states (eigenstates) to another (Wannier basis), which gives information about how many Planck cells each individual eigenstate occupies. We can reverse the unitary transformation and expand the Wannier basis in terms of the eigenstates; the expansion coefficients tell us not only how the Wannier basis forms the eigenstates, but more importantly how an initial state localized in the phase space will evolve for a long time. To illustrate this, we define the length $\mathcal{L}$ of a Planck cell $|\mathcal{X}, \mathcal{P}\rangle$ as

$$\mathcal{L} = \left(\sum_\phi |\langle \mathcal{X}, \mathcal{P}|\phi\rangle|^4 \right)^{-1}, \qquad (13)$$

which measures how much phase space $|\mathcal{X}, \mathcal{P}\rangle$ occupies in the spectrum. We have computed $\mathcal{L}$ for each Wannier function $|\mathcal{X}, \mathcal{P}\rangle$, and the results are plotted in Fig. 3(a), which resembles the classical Poincaré section that is divided into integrable and chaotic regions. Specifically, it is those Wannier bases in the classical integrable region that have small $\mathcal{L}$, while the others in the classical chaotic region have large $\mathcal{L}$.

Interestingly, the length $\mathcal{L}$ of a Planck cell $|\mathcal{X}, \mathcal{P}\rangle$ in fact also indicates how many Planck cells the system will explore dynamically if it starts at $|\mathcal{X}, \mathcal{P}\rangle$. To see this, we define the long-time area for a Planck cell $|\mathcal{X}, \mathcal{P}\rangle$ as

$$\mathcal{A}_{\text{orbit}} = \left(\left\langle \sum_{\mathcal{X}', \mathcal{P}'} |\langle \mathcal{X}', \mathcal{P}'|V^{n_T}|\mathcal{X}, \mathcal{P}\rangle|^4 \right\rangle_{n_T} \right)^{-1}. \qquad (14)$$

Here $\langle \cdot \rangle_{n_T}$ means taking the average of n_T, the number of periods. In practice, we use a diagonal ensemble to calculate this value (see Appendix B for details). In Fig. 3(b) we compare the $\mathcal{L}$ of each Wannier function $|\mathcal{X}, \mathcal{P}\rangle$ (dark blue dotted line) with its long-time area (light blue solid line). The sorted area of eigenstates (red solid line) is also plotted. The figure clearly shows that these three curves are close to each other, especially in the integrable part. These results
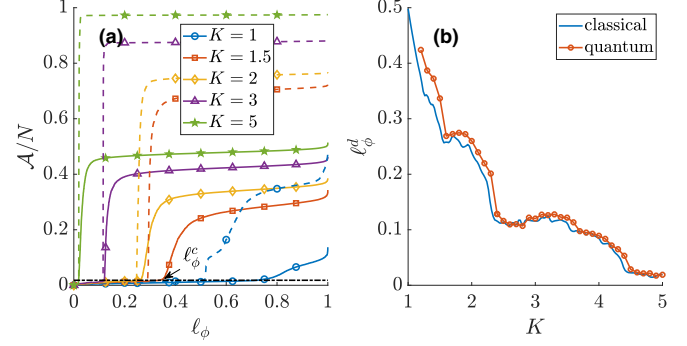

FIG. 4. (a) Area of each eigenstate (solid line) and coarse-grained area of classical trajectories (dashed line). (b) Demarcation point ℓ_ϕ^c for classical and quantum cases. Here ℓ_ϕ^c is obtained by $\mathcal{A}(\ell_\phi^c) = 0.018N$ and $\hbar_e = 2\pi/2^{14}$.

indeed show that the length $\mathcal{L}$ of a given Planck cell $|\mathcal{X}, \mathcal{P}\rangle$ measures how much phase space it will explore dynamically.

We now use the Wannier basis to study how the KAM effect breaks down for increasing K. Since the QKR becomes more chaotic as the kicking strength K increases, one expects that the critical value ℓ_ϕ^c decreases and eventually becomes zero. This is indeed the case as shown in Fig. 4, where we have also compared these results to their classical counterparts. For the classical results, we divide the phase space into $N = 100 \times 100$ cells, choose 10^4 random initial points, and evolve a long enough time ($n_T = 10^6$ kicks). Then each trajectory contains n_T points. For each trajectory, $\mathcal{A}$ is calculated similarly to the definition in the quantum case, $\mathcal{A} = [\sum_j (n_j/n_T)^2]^{-1}$, where n_j is the number of points in the jth cell. There is great consistency between the quantum results and the classical results. There are also differences. First of all, the saturation value of the classical $\mathcal{A}$ is much larger and close to the area of the chaotic sea in the phase space, which indicates that the chaotic sea is classically ergodic. The saturation value of the quantum $\mathcal{A}$ is smaller; this is due to the fact that the probability distribution of chaotic eigenstates on the phase space has large fluctuations [35]. Second, the classical demarcation point ℓ_ϕ^c differs from its quantum counterpart, which means there are more integrable eigenstates in the QKR than integrable trajectories in the CKR, especially when K is small. This is because there are hierarchial states which are supported by the chaotic region but behave like integrable states, as $\hbar_e$ is finite. Moreover, in the CKR the hierarchial regions of integrable islands are larger with smaller K.

B. Generic $\hbar_e$ and Anderson localization

In generic cases, $\hbar_e/2\pi$ is irrational and the matrix U cannot be reduced to a finite one. However, we can build a series of rational numbers $M_1/N_1, M_2/N_2, \ldots$, which has an irrational number $\hbar_e/2\pi$ as its limit. For each j, we have a resonant matrix U_j with effective Planck constant $\hbar_{e,j} = 2\pi M_j/N_j$, and we can do the previous reduction and construct the Wannier phase space. The properties of the system with the original $\hbar_e$ are approximated by increasing j.
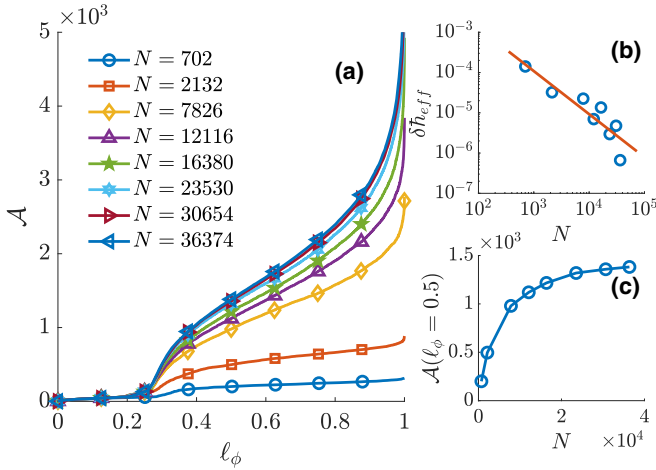
FIG. 5. (a) Area $\mathcal{A}$ of eigenstates for each j. (b) Rational approximation of generic $\hbar_e$. For each j, $\delta\hbar_e \equiv |\hbar_e - \hbar_{e,j}|$. (c) Area $\mathcal{A}$ at $\phi = 0.5$, which saturates when $N \to \infty$. The parameters are $K = 2$, $N_x = 26$, and $\Delta = 1/\sqrt{2}$; the index j is omitted.

Without loss of generality, we let $\hbar_e = 2\pi/(N_x + \Delta)^2$, where N_x is an even integer and $\Delta \in [-1, 1)$ is irrational. Then we construct a series $\{M_j/N_x N_{p,j}\}$ such that the series $\{M_j/N_{p,j}\}$ approaches $N_x/(N_x + \Delta)^2$. For this series, the quantum phase space has $N_j = N_x N_{p,j}$ Wannier states in total.

In Fig. 5 we plot the rational approximation of $\hbar_e$ and the area of eigenstates for each j. The area of integrable eigenstates remains a small constant when N increases, because each eigenstate is confined in one integrable island of one sub-phase-space, which contains a constant number of Planck cells. On the other hand, the area of chaotic eigenstates increases with N when N is small and saturates when N is large enough. The initial growth is consistent with the classical version, in which the chaotic regions of each sub-phase-space are connected and one point can transport freely in the chaotic sea of the whole phase space. However, the effect of Anderson localization comes in when N is sufficiently large [36], which is a pure quantum effect and sets an upper bound of $\mathcal{A}$. To be specific, the localization length in p space of each eigenstate is approximately $n_{\text{loc}} = \frac{1}{2}D_c/\hbar_e^2$, where D_c is the classical diffusion coefficient [37]. If $N > n_{\text{loc}}$, although the chaotic eigenstates are not confined in one integrable island, they are localized in some part of the phase space, whose area is of the order of n_{loc} and independent of N.

For a one-step evolution matrix U with generic $\hbar_e$, we can also simply set a large momentum cutoff n_{cut} ($\gg n_{\text{loc}}$) and only consider those eigenstates which are localized in the center of the whole p space. These states have a small truncation error, and we are able to apply the Wannier basis analysis to them. The quantum phase space can be constructed as follows. Choose $N = N_x N_p$ adjacent momentum eigenstates $|n_0 + 1\rangle, \ldots, |n_0 + N\rangle$, relabel them as $|1\rangle, \ldots, |N\rangle$, and apply Eq. (7) to generate the Wannier basis which constitutes the phase space. The ambiguity here is that the phase space depends on n_0, which is insignificant because the change of n_0 only causes a slight displacement of Planck cells in the phase space. In a similar manner, we can project the eigenstates
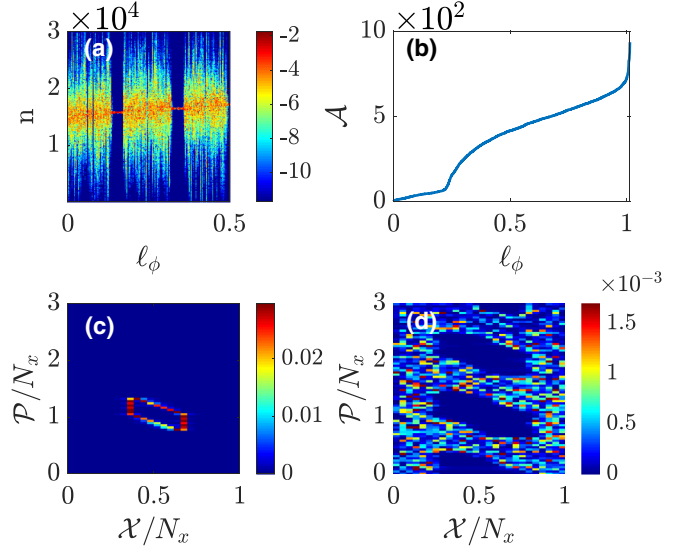

FIG. 6. Eigenstates of U with generic $\hbar_e$ without reduction. After diagonalization, we choose only $\sim 2 \times 10^3$ eigenstates ϕ whose average momentum $\langle n \rangle \sim 1.5 \times 10^4$, where the whole p space is $1 \leqslant n \leqslant 3 \times 10^4$. The quantum phase space is constructed by $3N_x^2$ adjacent momentum eigenstates near $n \sim 1.5 \times 10^4$, where $N_x = 26$, $\hbar_e = 2\pi/(N_x + \Delta)^2$, $\Delta = 1/\sqrt{2}$, and $K = 2$. (a) Plot of $\ln |\langle n|\phi\rangle|^2$. (b) Area of eigenstates. The value of $\mathcal{A}$ is normalized by the projection of each eigenstate to the phase space: $\mathcal{A}(\phi) = \frac{[\sum_{\mathcal{X},\mathcal{P}} |\langle \mathcal{X},\mathcal{P}|\phi\rangle|^2]^2}{\sum_{\mathcal{X},\mathcal{P}} |\langle \mathcal{X},\mathcal{P}|\phi\rangle|^4}$. (c) One typical integrable eigenstate in quantum phase space. (d) One typical chaotic eigenstate in quantum phase space.

onto the phase space we have constructed. In Fig. 6 we show that these eigenstates are also separated into integrable and chaotic ones, which justifies that this structure of eigenstates depends on neither the previous rational approximation nor the reduction process.

IV. CONCLUSION

We have developed a method based on Wannier phase space to approach the KAM effect in quantum systems. In this approach, each Planck cell in the quantum phase space is represented by a Wannier function; all the Wannier functions together form a complete and orthonormal basis. With the example of the QKR, this approach has been shown to be quite powerful. First, it has led us to define the area and effective dimension of eigenstates, which then give us quantitative measures to divide all eigenstates into integrable and chaotic classes. Second, it has allowed us to define the length of each Planck cell, which measures quantitatively how many Planck cells the system will traverse if it starts at one Planck cell. Third, this approach is also used to clarify the distinction between the KAM effect and Anderson localization in the QKR. We have used this approach in systems with a classical limit, and it is interesting to consider whether it can be generalized to other quantum systems like spin chains. This work complements our understanding of the quantum-classical correspondence and may provide insight into short-wavelength physics such as microcavity photonics.

APPENDIX A: QUANTUM RESONANCE IN THE QKR

1. Classical origin of translational invariance

The existence of quantum resonance in the QKR relies on the emergence of a translational invariance in p space, which can be understood in the classical limit [27]. The classical kicked rotor is described by a pair of classical conjugate variables (x_c, p_c). Its dynamics is an iterating map

$$p_c' = p_c + K_c \sin(2\pi x_c), \tag{A1}$$

$$2\pi x_c' = 2\pi x_c + p_c'. \tag{A2}$$

This map is invariant under the transformation $p_c \to p_c + 2\pi M_c$, where M_c is an integer. In the QKR, the angular momentum p_c is quantized, that is, $p_c = m\hbar_e$. Thus the transformation becomes $m\hbar_e + 2\pi M_c = m'\hbar_e$, where m, m', and M_c are integers. It is clear that for the QKR to be invariant under this transformation, $\hbar_e/2\pi$ has to be rational.

2. Existence of Bloch states

We use here group theory to show the existence of the Bloch states in p space in the QKR under the condition $U_{n+N\ell, n'+N\ell} = U_{nn'}$ ($l = 0, \pm 1, \ldots$), that is, to prove Eqs. (4)–(6). Let $\mathcal{T}$ be the operator that translates the system in p space by N, $\mathcal{T}|n\rangle = |n + N\rangle$. One can prove that $(\mathcal{T}U\mathcal{T}^{-1})_{nn'} = U_{n-N,n'-N} = U_{nn'}$, indicating that the QKR has a translational symmetry $\mathcal{T}$ in p space, similar to the translational symmetry in x space for crystal. All operators of the type $\mathcal{T}^k$, where k is an integer, form a symmetry group. Since it is Abelian, each eigenstate $|\phi\rangle$ of U is a one-dimensional irreducible representation of the group. That suggests that $\mathcal{T}|\phi\rangle = e^{-i\theta}|\phi\rangle$ for some $\theta \in [0, 2\pi)$, which leads to Eq. (4).

Consider the eigenequation $\sum_{n'} U_{nn'}\phi(n') = e^{-i\omega_\phi}\phi(n)$. With Eq. (4) we have, for $s = 1, \ldots, N$,

$$
\begin{aligned}
e^{-i\omega_\phi}\phi(s) &= \sum_{n'=-\infty}^{\infty} U_{sn'}\phi(n') \\
&= \sum_{s'=1}^{N} \sum_{l'=-\infty}^{\infty} U_{s(s'+Nl')}\phi(s'+Nl') \\
&= \sum_{s'=1}^{N} \sum_{l'=-\infty}^{\infty} U_{s(s'+Nl')}e^{-il'\theta}\phi(s').
\end{aligned} \tag{A3}
$$

This is just Eqs. (5) and (6).

APPENDIX B: LONG-TIME AREA

In this Appendix we provide the details of calculating the long-time area of evolved states by a diagonal ensemble. Here we consider a general initial state $|\psi_0\rangle = \sum_\phi a_\phi|\phi\rangle$, while previous results are for the special case $|\psi_0\rangle = |\mathcal{X}, \mathcal{P}\rangle$. Its inverse area after n_T periods is given by

$$
\begin{aligned}
\mathcal{A}^{-1}(n_T) &= \sum_{\mathcal{X}', \mathcal{P}'} |\langle \mathcal{X}', \mathcal{P}'|U^{n_T}|\psi_0\rangle|^4 \\
&= \sum_{\mathcal{X}', \mathcal{P}'} \sum_{\phi_1, \phi_2, \phi_1', \phi_2'} e^{-in_T(\omega_{\phi_1}+\omega_{\phi_2}-\omega_{\phi_1'}-\omega_{\phi_2'})} \\
&\quad \times a_{\phi_1}a_{\phi_2}a_{\phi_1'}^*a_{\phi_2'}^* \langle \mathcal{X}', \mathcal{P}'|\phi_1\rangle \langle \mathcal{X}', \mathcal{P}'|\phi_2\rangle \\
&\quad \times \langle \mathcal{X}', \mathcal{P}'|\phi_1'\rangle^* \langle \mathcal{X}', \mathcal{P}'|\phi_2'\rangle^*.
\end{aligned} \tag{B1}
$$

Then one can take the average of n_T,

$$
\begin{aligned}
&\langle e^{-in_T(\omega_{\phi_1}+\omega_{\phi_2}-\omega_{\phi_1'}-\omega_{\phi_2'})}\rangle_{n_T} \\
&= \delta_{\phi_1\phi_1'}\delta_{\phi_2\phi_2'} + \delta_{\phi_1\phi_2'}\delta_{\phi_2\phi_1'},
\end{aligned} \tag{B2}
$$

by assuming that there is no degeneracy in the differences of quasienergies, which is the case for the QKR. Finally, one gets the diagonal ensemble value

$$
\begin{aligned}
\mathcal{A}_{\text{orbit}}^{-1} = 2\sum_{\mathcal{X}', \mathcal{P}'} &\left(\sum_\phi |a_\phi|^2 |\langle \mathcal{X}', \mathcal{P}'|\phi\rangle|^2 \right)^2 \\
&- \sum_{\mathcal{X}', \mathcal{P}'} \sum_\phi |a_\phi|^4 |\langle \mathcal{X}', \mathcal{P}'|\phi\rangle|^4.
\end{aligned} \tag{B3}
$$

[1] V. I. Arnold, *Mathematical Methods of Classical Mechanics*, Graduate Texts in Mathematics Vol. 60 (Springer Science + Business Media, New York, 1978).

[2] M. C. Gutzwiller, *Chaos in Classical and Quantum Mechanics*, Interdisciplinary Applied Mathematics Vol. 1 (Springer, New York, 1990).

[3] A. N. Kolmogorov, Dokl. Akad. Nauk. SSSR **98**, 527 (1954).

[4] J. K. Möser, Nach. Akad. Wiss. Göttingen, Math. Phys. Kl. II **1962**, 1 (1962).

[5] V. I. Arnold, Russ. Math. Surv. **18**, 9 (1963).

[6] G. Hose and H. S. Taylor, Phys. Rev. Lett. **51**, 947 (1983).

[7] G. Hose, H. S. Taylor, and A. Tip, J. Phys. A: Math. Gen. **17**, 1203 (1984).

[8] T. Geisel, G. Radons, and J. Rubner, Phys. Rev. Lett. **57**, 2883 (1986).

[9] L. E. Reichl and W. A. Lin, Found. Phys. **17**, 689 (1987).

[10] W. A. Lin and L. E. Reichl, Phys. Rev. A **37**, 3972 (1988).

[11] L. C. Evans, Commun. Math. Phys. **244**, 311 (2004).

[12] B. Grébert and L. Thomann, Commun. Math. Phys. **307**, 383 (2011).

[13] A. Polkovnikov, K. Sengupta, A. Silva, and M. Vengalattore, Rev. Mod. Phys. **83**, 863 (2011).

[14] G. P. Brandino, J.-S. Caux, and R. M. Konik, Phys. Rev. X **5**, 041043 (2015).

[15] I. C. Percival, J. Phys. B **6**, L229 (1973).

[16] A. Voros, Annales de l'I.H.P. Phys. théorique **24**, 31 (1976).

[17] M. V. Berry, J. Phys. A: Math. Gen. **10**, 2083 (1977).

[18] M. V. Berry, in *Chaotic Behaviour of Deterministic Systems*, edited by G. Iooss, R. H. G. Helleman, and R. Stora, Proceedings of the Les Houches Summer School of Theoretical Physics, XXXVI, 198 (North-Holland, Amsterdam, 1983), p. 171.

[19] A. Voros, in *Stochastic Behavior in Classical and Quantum Hamiltonian Systems*, edited by G. Casati and J. Ford, Lecture Notes in Physics Vol. 93 (Springer, Berlin, 1979), pp. 326–333.

[20] E. J. Heller, Phys. Rev. Lett. **53**, 1515 (1984).

[21] K. Zyczkowski, Phys. Rev. A **35**, 3546 (1987).

[22] R. Ketzmerick, L. Hufnagel, F. Steinbach, and M. Weiss, Phys. Rev. Lett. **85**, 1214 (2000).

[23] X. Han and B. Wu, Phys. Rev. E **91**, 062106 (2015).

[24] Y. Fang, F. Wu, and B. Wu, J. Stat. Mech. (2018) 023113.

[25] J. Jiang, Y. Chen, and B. Wu, arXiv:1712.04533.

[26] B. V. Chirikov, Phys. Rep. **52**, 263 (1979).

[27] S.-J. Chang and K.-J. Shi, Phys. Rev. A **34**, 7 (1986).

[28] G. Casati, B. V. Chirikov, F. M. Izraelev, and J. Ford, in *Stochastic Behavior in Classical and Quantum Hamiltonian Systems*, edited by G. Casati and J. Ford, Lecture Notes in Physics, Vol. 93 (Springer, Berlin, Heidelberg, 1979), pp. 334–352.

[29] B. Chirikov and D. Shepelyansky, Scholarpedia **3**, 3550 (2008).

[30] P. Jacquod and D. L. Shepelyansky, Phys. Rev. Lett. **75**, 3501 (1995).

[31] Y. V. Fyodorov and A. D. Mirlin, Phys. Rev. B **52**, R11580 (1995).

[32] B. Georgeot and D. L. Shepelyansky, Phys. Rev. Lett. **79**, 4365 (1997).

[33] F. Haake, *Quantum Signatures of Chaos*, 2nd ed., Springer Series in Synergetics Vol. 54 (Springer, Berlin, 2010).

[34] M. Heyl, P. Hauke, and P. Zoller, Sci. Adv. **5**, eaau8342 (2019).

[35] H. W. Xiong and B. Wu, Laser Phys. Lett. **8**, 398 (2011).

[36] D. R. Grempel, R. E. Prange, and S. Fishman, Phys. Rev. A **29**, 1639 (1984).

[37] D. L. Shepelyansky, Phys. Rev. Lett. **56**, 677 (1986).